Hydration Structure of Na^+ in Concentrated Aqueous Solutions

Yasuo Kameda,* Kentaro Sugawara, Takeshi Usuki, and Osamu Uemura

Department of Material and Biological Chemistry, Faculty of Science, Yamagata University, Yamagata 990-8560

(Received April 21, 1998)

X-Ray diffraction and Raman spectroscopic measurements have been carried out for aqueous 10 mol% NaX (X = Cl, Br, ClO_4, and NO_3) solutions in order to determine the hydration structure of Na^+ in concentrated aqueous solutions. Isotropic Raman spectra for NaX–H_2O solutions exhibit a polarized peak centered at 183—187 cm^{-1}. The corresponding peak in the isotropic spectra for NaX–D_2O solutions is shifted to the lower frequency side by ca. 10 cm^{-1}, indicating that the peak can be assigned to the totally symmetric vibrational mode of hydrated Na^+, $Na^+(H_2O)_n$. The least-squares fitting analysis was applied to the X-ray interference term observed for these solutions in order to discuss the hydration number of Na^+ in concentrated aqueous solutions.

The hydration structure around Na^+ in the solution has long been a matter of interest in extended fields of chemistry and biology. Despite considerable efforts for elucidating the structural property of hydrated Na^+ in the aqueous solution, there still remain ambiguities concerning the number of solvent molecules neighboring to Na^+ as well as the effect of coexisting counter anion on the hydration geometry of the ion.

Earlier X-ray diffraction studies have not been able to distinguish sufficiently the $Na^+\cdots H_2O$ correlation out of the total radial distribution function.[1,2] Recent X-ray diffraction studies, involving the least-squares fitting analysis to the observed interference term, have revealed that the nearest-neighbor $Na^+\cdots H_2O$ distance falls in the range 2.37—2.42 Å.[3—10] On the other hand, Caminiti et al. have reported relatively longer values of the distance, such as 2.44 and 2.49 Å, in concentrated aqueous $NaNO_3$ solutions.[11] Further, the difference method of neutron and X-ray diffraction intensities has given 2.5[12] and 2.40 Å[13] as this distance. The hydration number of Na^+ in the aqueous solution hitherto determined by diffraction studies scatters between 4 and 8.

According to the computer simulation results, the $Na^+\cdots H_2O$ distance lies in the 2.30—2.36 Å range.[14—17] Such values are slightly smaller than those observed by neutron and X-ray diffraction studies. The hydration number of Na^+ in the aqueous solution, reported by computer simulation studies, is close to 6. After all, it seems at present that there still remain some problems about the hydration structure around Na^+ in the aqueous solution.

Vibrational spectroscopic studies also provide important structural information with respect to the hydration structure around the metal ion. In liquid pure water, the intermolecular hydrogen-bonded stretching band has been known to appear at $\nu \approx 180$ cm^{-1} in infrared and Raman spectra.[21—29] The effect of solute ions, as well as the solute concentration, to the 180 cm^{-1} band in the aqueous solution has been extensively examined.[18,21,22,25,28] If H_2O molecules in the first hydration shell of the metal ion prefer to take a given stable configuration such as $M^{m+}(H_2O)_n$, the totally symmetric stretching vibrational mode (ν_1) of the hydrated structural unit should be observed as a highly polarized Raman band in the low frequency region. In fact, the ν_1 mode of various hydrated transition metal ions in the aqueous solution has been observed in Raman spectroscopic studies.[30—35] On the other hand, only a few results of the ν_1 mode have been reported on hydrated alkali metal ions in the solution. Michaelian and Moscovits have reported some indications for the ν_1 mode of hydrated Li^+ and Na^+ in the aqueous solution applying the difference method of Raman scattering intensities.[36] More recently, the ν_1 mode of hydrated Li^+ has been independently reported by Kameda et al.[37] and Rudolph et al.[38] Nevertheless, no unambiguous evidence for the symmetric stretching vibrational mode of hydrated Na^+, $Na^+(H_2O)_n$, in the aqueous solution has yet been presented. Experts consider that more polarized modes such as the totally symmetric stretching mode would strongly appear in the isotropic Raman spectrum, while less polarized modes such as deformation and anti-symmetric stretching modes would disappear. Therefore, isotropic Raman spectroscopic studies would supply more detailed information on the $Na^+\cdots H_2O$ symmetrical stretching mode of hydrated Na^+ in the aqueous solution.

In this paper we describe results of low-frequency isotropic Raman spectra in aqueous 10 mol% NaX (X: Cl, Br, ClO_4, and NO_3) solutions to determine corrected vibrational frequencies for hydrated Na^+ in the concentrated aqueous solutions. Simultaneous measurements on NaX–D_2O solutions with the corresponding H_2O solutions have also been made to confirm the assignment of the $Na^+\cdots H_2O$ stretching vibrational mode of hydrated Na^+. Moreover, X-ray diffraction measurements of the corresponding solutions have been added in order to determine the hydration number of Na^+ in the concentrated aqueous solution and to investigate the influence of the anion substitution.

Experimental

Raman Scattering Measurements. Aqueous 10 mol% NaX (X: Br, ClO_4, and NO_3) solutions were prepared by dissolving weighted amounts of anhydrous salts (Nacalai tesque, Guaranteed grade) into distilled H_2O and into D_2O (Aldrich Chemical Co., Inc., 99.9% D). For the NaCl solution, the composition of the sample solution was selected just below the solubility limit at 25 °C, i.e., 9.8 mol% NaCl in the H_2O solution and 9.3 mol% NaCl in the D_2O solution, respectively. All solutions were filtered through a 0.45 μm Teflon® millipore filter before introducing them into a Pyrex® Raman cell (10×10 mm and 40 mm H) so as to remove any dust particles. The polarized Raman spectrum was recorded at 25 °C in the frequency range of $30 \leq \nu \leq 1000$ cm^{-1} using a JASCO NR-1100 spectrometer with a 514.5 nm line of an NEC GLG-3200 Ar^+ laser operated at 200 mW. The calibration of the monochromator was made using 89 of the neon emission lines. The efficiency of the polarization filter was carefully checked through the measurement of the depolarization ratio of ν_1, ν_2, and ν_4 bands of CCl_4 molecule in the liquid state. The details concerning the Raman scattering measurement are completely identical with those described in our previous papers.[37,39]

X-Ray Diffraction Measurements. The X-ray diffraction intensity with Mo $K\alpha$ radiation (λ = 0.7107 Å) was measured at 25 °C under the reflection geometry using a θ–θ X-ray diffractometer manufactured by Rigaku Co. Scattered X-ray intensities from the sample solution were counted at the interval of 0.2° over the angular range of $3 \leq 2\theta \leq 150°$, corresponding to the range of scattering vector magnitude: $0.5 \leq Q \leq 17.1$ Å^{-1} ($Q = 4\pi \sin\theta/\lambda$), with a fixed counting time of 100 s. The whole angular range was scanned four times to keep good statistics for the diffraction data, and to minimize any long-term intensity drift. The total number of counts per one data point reached at least 10^5. The details concerning the X-ray diffraction measurement have previously been described.[9]

Data Reduction

Raman Scattering Data. The correction of the Bose–Einstein factor for observed Raman spectra, which is needed to distinguish low-frequency components, was made using the following equation:[24,40—42]

$$I^{\text{corrected}}(\nu) = (\nu_0 - \nu)^{-4} \cdot \nu \cdot [1 - \exp(-h\nu/kT)] \cdot I^{\text{obs}}(\nu), \quad (1)$$

where, ν_0 and ν are the Stokes–Raman shift and frequency of the incident light, respectively. T corresponds to the absolute temperature. The isotropic Raman intensity, $I^{\text{iso}}(\nu)$, can be given using

$$I^{\text{iso}}(\nu) = I^{//}(\nu) - (4/3)I^{\perp}(\nu), \quad (2)$$

where, $I^{//}(\nu)$ and $I^{\perp}(\nu)$ denote corrected parallel and perpendicular spectra, respectively. The peak analysis of the isotropic spectra was performed with the SALS program,[43] assuming a Gaussian peak function.

X-Ray Diffraction Data. The correction and normalization procedures for observed X-ray diffraction intensities were very similar to those described in our previous paper.[9] The observed X-ray total interference term, $i^{\text{total}}(Q)$, scaled by the stoichiometric unit, $(NaX)_x(H_2O)_{1-x}$, can be expressed as

$$i^{\text{total}}(Q) = (I_{\text{eu}}(Q) - \langle f^2 \rangle)/\langle f \rangle^2, \quad (3)$$

where

$$\langle f^2 \rangle = \sum c_i [(f_i(Q) + f_i')^2 + f_i''^2] \quad (4)$$

and

$$\langle f \rangle^2 = [\sum c_i (f_i(Q) + f_i')]^2 + [\sum c_i f_i'']^2, \quad (5)$$

respectively. Here, $I_{\text{eu}}(Q)$ gives the normalized coherent scattering intensity in electron units. c_i and $f_i(Q)$ correspond to the number of atom i within the stoichiometric unit and atomic scattering factor of atom i, respectively. Real and imaginary parts of the anomalous dispersion factor are respectively shown by f_i' and f_i''. The distribution function, $g(r)$, can be evaluated by the following Fourier transform of $i(Q)$ with the upper integral limit of Q, $Q_{\max}$ = 17.1 Å^{-1}:

$$g(r) = 1 + (2\pi^2 \rho r)^{-1} \int_0^{Q_{\max}} Q i(Q) \sin(Qr) \mathrm{d}Q, \quad (6)$$

where ρ is the number density of the stoichiometric unit, $(NaX)_x(H_2O)_{1-x}$.

The observed total interference term, $i^{\text{total}}(Q)$, can be divided into two contributions, namely, the intra- and intermolecular interference terms:

$$i^{\text{total}}(Q) = i^{\text{intra}}(Q) + i^{\text{inter}}(Q). \quad (7)$$

For the NaCl and NaBr solutions,

$$i^{\text{intra}}(Q) = (1 - x) \cdot i^{\text{intra}}(Q) \quad (\text{for } H_2O), \quad (8)$$

for the $NaClO_4$ solution,

$$i^{\text{intra}}(Q) = x \cdot i^{\text{intra}}(Q) \ (\text{for } ClO_4^-) + (1 - x) \cdot i^{\text{intra}}(Q) \ (\text{for } H_2O) \quad (9)$$

and for the $NaNO_3$ solution,

$$i^{\text{intra}}(Q) = x \cdot i^{\text{intra}}(Q) \ (\text{for } NO_3^-) + (1 - x) \cdot i^{\text{intra}}(Q) \ (\text{for } H_2O), \quad (10)$$

respectively. The intramolecular interference terms for H_2O, ClO_4^-, and NO_3^- are respectively written as below:

$$\begin{aligned} i^{\text{intra}}(Q) \ (\text{for } H_2O) &= 4[(f_O(Q) + f_O')(f_H(Q) + f_H') + f_O'' f_H''] \\ &\times \exp(-l_{OH}^2 Q^2/2) \sin(Qr_{OH})/(Qr_{OH}) + 2[(f_H(Q) + f_H')^2 + f_H''^2] \\ &\times \exp(-l_{HH}^2 Q^2/2) \sin(Qr_{HH})/(Qr_{HH}), \end{aligned} \quad (11)$$

$$\begin{aligned} i^{\text{intra}}(Q) \ (\text{for } ClO_4^-) &= 8[(f_{Cl}(Q) + f_{Cl}')(f_O(Q) + f_O') + f_{Cl}'' f_O''] \\ &\times \exp(-l_{ClO}^2 Q^2/2) \sin(Qr_{ClO})/(Qr_{ClO}) \\ &+ 12[(f_O(Q) + f_O')^2 + f_O''^2] \exp(-l_{OO}^2 Q^2/2) \sin(Qr_{OO})/(Qr_{OO}), \end{aligned} \quad (12)$$

and

$$\begin{aligned} i^{\text{intra}}(Q) \ (\text{for } NO_3^-) &= 6[(f_N(Q) + f_N')(f_O(Q) + f_O') + f_N'' f_O''] \\ &\times \exp(-l_{NO}^2 Q^2/2) \sin(Qr_{NO})/(Qr_{NO}) + 6[(f_O(Q) + f_O')^2 + f_O''^2] \\ &\times \exp(-l_{OO}^2 Q^2/2) \sin(Qr_{OO})/(Qr_{OO}), \end{aligned} \quad (13)$$

respectively. Here, l_{ij} and r_{ij} denote the root-mean-square amplitude and interatomic distance of i–j pairs. The theoretical intermolecular interference term, $i^{\text{inter}}(Q)$, was calculated

by the sum of the nearest-neighbor short-range interaction, $i^{s}(Q)$, and long-range interaction, $i^{l}(Q)$, for all possible atom pairs in the solution,

$$i^{inter}(Q) = i^{s}(Q) + i^{l}(Q), \tag{14}$$

where

$$i^{s}(Q) = \sum i_{ij}(Q), \tag{15}$$

and

$$i_{ij}(Q) = (2 - \delta_{ij})c_{ij}n_{ij}[(f_i(Q) + f_i')(f_j(Q) + f_j') + f_i''f_j''] \times \exp(-l_{ij}^2Q^2/2)\sin(Qr_{ij})/(Qr_{ij})/\langle f\rangle^2. \tag{16}$$

$$\begin{cases} \delta_{ij} = 1 \ (i = j) \\ \delta_{ij} = 0 \ (i \neq j). \end{cases}$$

The long-range interaction was evaluated using the following equation:[8,44,45]

$$i^{l}(Q) = 4\pi\rho\sum c_ic_j[(f_i(Q) + f_i')(f_j(Q) + f_j') + f_i''f_j''] \times \exp(-l_{0ij}^2Q^2/2)[Qr_{0ij}\cos(Qr_{0ij}) - \sin(Qr_{0ij})]Q^{-3}/\langle f\rangle^2, \tag{17}$$

where, r_{0ij} denotes the distance beyond which the continuous distribution of j atoms around atom i is assumed. The parameter l_{0ij} describes the sharpness of the boundary at r_{0ij}. Parameters n_{ij}, l_{ij}, and r_{ij} in Eq. 16, and l_{0ij} and r_{0ij} in Eq. 17 were respectively determined through the least-squares fit of $i^{total}(Q)$ (Eq. 7) to the observed $i^{obs}(Q)$. The fitting procedure was performed in the range of $1.0 \leq Q \leq 17.1$ Å^{-1} with the SALS program.[43]

Results and Discussion

Observed isotropic Raman spectra for aqueous 10 mol% NaX–H_2O solutions are shown in Fig. 1, in which the isotropic spectrum for pure H_2O is also included for comparison. There seem to be no significant peaks in the range of $\nu < 300$ cm^{-1} in the spectrum for pure H_2O. On the other hand, a broad peak at ca. 180 cm^{-1} is obvious in the spectra for all NaX solutions, indicating that this peak has arisen from the solute–solvent (i.e., ion–water) interaction in these solutions. Since isotropic Raman spectra involve vibrational modes with the higher symmetry, this peak may be ascribed to the symmetric stretching mode of the hydrated ion in the aqueous solution, that is to say, the peak at ca. 180 cm^{-1} can be assigned to the symmetric stretching mode of the hydrated Na^+, $Na^+(H_2O)_n$, in the NaX solution because of the anion-independent peak position. The peak position, full-width at the half maximum, and peak height were each determined by the Gaussian decomposition to the peak components based on the least-squares fitting procedure. The background function was approximated by the polynomial function defined below:

$$I^{bg}(\nu) = a\nu^3 + b\nu^2 + c\nu. \tag{18}$$

In the present procedure, at least two Gaussian components was found to be necessary for reproducing the total peak shape in the spectra for the NaBr, $NaClO_4$, and $NaNO_3$ solutions, respectively, while three Gaussian components were necessary for the NaCl solution. Results of the least-squares fitting procedure are summarized in Table 1. In all solutions the position of Peak 2 falls at almost the same value, 183—187 cm^{-1}, while that of Peak 1 has various frequencies depending on the anion. The value of the full-width at the half maximum of Peak 2 remains in good agreement for all the present solution. Considering that Na^+ is the common chemical species in these solutions, Peak 2 can be attributed to the totally symmetric stretching vibrational mode of hydrated Na^+, $Na^+(H_2O)_n$. If this might be the case, the vibrational frequency of this mode should be shifted to the lower frequency side by substituting solvent molecules from H_2O ($m_{H_2O} = 18$) to D_2O ($m_{D_2O} = 20$). Observed isotropic Raman spectra for the NaX–D_2O solutions are given in Fig. 2. The result of the Gaussian decomposition for the NaX–D_2O solutions is included in Table 1. The general features of the spectra for the D_2O solution seem very similar to those for the H_2O solution. However, only the position of Peak 2 for the D_2O solution indicates a systematic shift to the lower frequency side by 8—13 cm^{-1} comparing with that for the corresponding NaX–H_2O solution. The position of Peaks 1 and 3 exhibits no systematic frequency shift due to the H/D substitution. If we assume a highly symmetrical structure for hydrated Na^+ such as tetrahedral ($n = 4$) or octahedral ($n = 6$) geometries, the ratio of the ν_1 frequency for the H_2O solution to that for the D_2O solution can be roughly calculated by the following equation:

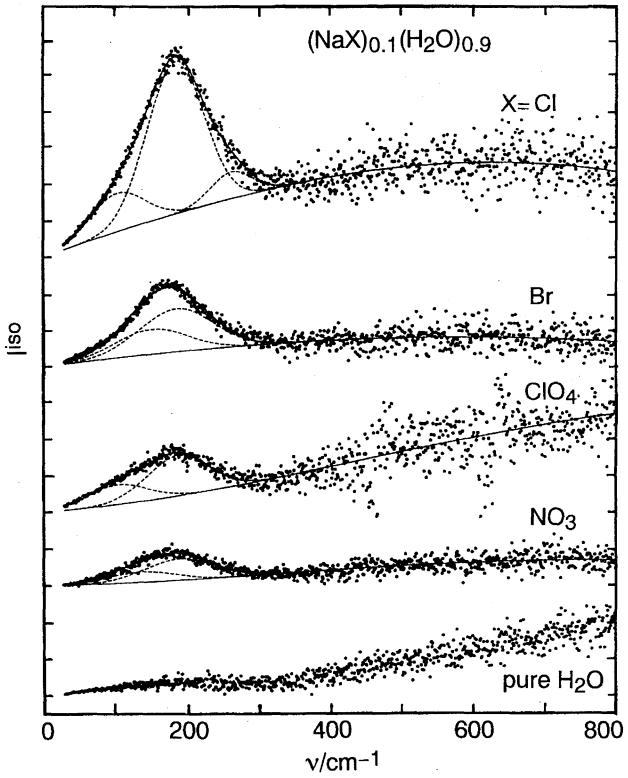

Fig. 1. The isotropic Raman spectra for aqueous 10 mol% NaX (X: Cl, Br, ClO_4, and NO_3) solutions in H_2O at 25 °C. The Gaussian components derived from the least-squares fit are indicated by broken lines.

Table 1. The Peak Position, Full Width at Half Maximum, and Peak Height of Gaussian Components Derived from the Least Squares Fit of the Isotropic Raman Spectra for Aqueous $(NaX)_x(Z_2O)_{1-x}$ Solutions, ν, w, and h, Respectively[a)]

			Peak 1			Peak 2			Peak 3		
X	x	Z	ν/cm^{-1}	w/cm^{-1}	h	ν/cm^{-1}	w/cm^{-1}	h	ν/cm^{-1}	w/cm^{-1}	h
Cl	0.098	H	100.2(1)	88.4(3)	1.05(1)	182.7(1)	91.4(1)	4.23(1)	260.2(2)	68.5(5)	0.73(1)
	0.093	D	100.5(1)	66.5(8)	0.40(1)	174.3(1)	94.4(1)	3.38(1)	261.6(3)	98.8(6)	0.71(1)
Br	0.100	H	150(5)	115(13)	0.69(9)	183(3)	119(6)	1.20(9)			
	0.100	D	152(13)	107(12)	0.31(9)	172(6)	116(5)	0.72(9)			
ClO_4	0.100	H	101.6(4)	97.6(9)	0.54(1)	185.3(2)	101.2(4)	1.11(1)			
	0.100	D	101.5(1)	90(1)	0.32(1)	172.6(3)	93.8(5)	0.80(1)			
NO_3	0.100	H	135(6)	107(12)	0.56(4)	187(3)	117(6)	1.15(4)			
	0.100	D	129(7)	114(15)	0.51(5)	176(4)	94(8)	0.82(6)			

a) Estimated standard deviations are given in parentheses.

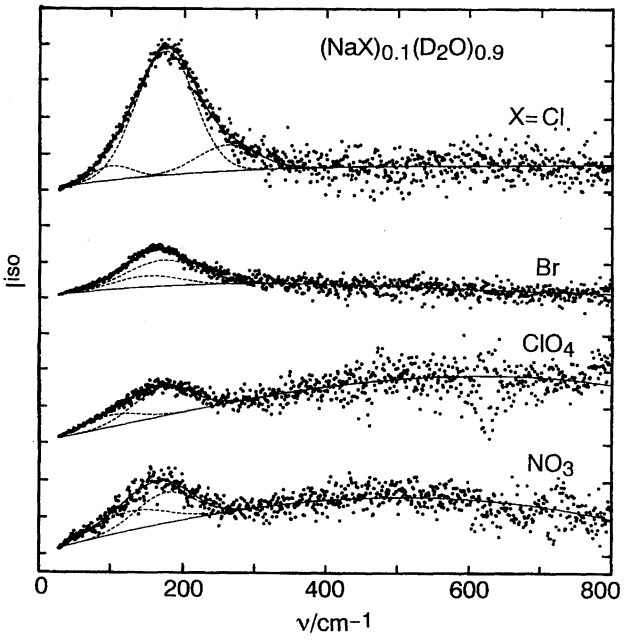

Fig. 2. Same notations as in Fig. 1, except for the heavy water solutions, $(NaX)_{0.1}(D_2O)_{0.9}$.

$$\nu_{D_2O\ soln}/\nu_{H_2O\ soln} \approx (m_{H_2O}/m_{D_2O})^{1/2} = 0.95. \quad (19)$$

The calculated value corresponds well to the frequency ratio, 0.93—0.95, observed for Peak 2 in the present NaX solutions by which we support the band assignment in this study as reasonable. Therefore, the hydrated structure around Na^+ appears to have high symmetry even in such a concentrated aqueous solution.

It is generally difficult to obtain the absolute scattering intensity in Raman scattering measurements; however, the observed scattering intensities for $NaClO_4$ and $NaNO_3$ solutions in the low frequency region, are quite weak compared with those for NaCl and NaBr solutions. The reason is not clear at present. The low-frequency isotropic Raman band is known to be sensitive to the ion-pair formation in the aqueous solution. Previous results of highly concentrated aqueous LiX solutions (X: Cl and Br) indicated some evidence for the stretching vibrational band of hydrated ion-pair, $Li^+X^-(H_2O)_n$, which is observed as an independent peak located at higher-frequency side of the symmetrical stretching band of the hydrated Li^+, $Li^+(H_2O)_n$.[37,38] In the present isotropic Raman spectra for aqueous 10 mol% NaX solutions, no indication of the vibrational mode of the $Na^+X^-(H_2O)_n$, can be observed, implying that the concentration of the ion-pair is small in the present solutions. Furthermore, the ν_1 frequency of $Na^+(H_2O)_n$ in the present solutions exhibits almost the same value within the experimental errors, suggesting that the hydration structures of Na^+ in the present solutions are all similar.

The hydration number of Na^+, n, was analyzed through the least-squares fit to the observed X-ray interference term in the present NaX solutions. The observed X-ray interference term and radial distribution function are represented in Figs. 3 and 4, respectively. The short-range peak at ca. 1 Å in $g^{total}(r)$ for the NaCl and NaBr solutions is assigned to the intramolecular O–H correlation within a H_2O molecule. For $NaClO_4$ and $NaNO_3$ solutions, intramolecular contributions from ClO_4^- and NO_3^- as well as H_2O molecule are respectively subtracted from the observed total interference terms before the fitting analysis, to reduce the number of independent parameters in the fitting procedure and to obtain reliable intermolecular structure parameters. The intramolecular structure parameters employed for the H_2O molecule are $r_{OH} = 0.983$ Å, $l_{OH} = 0.062$ Å, $r_{HH} = 1.55$ Å, and $l_{HH} = 0.12$ Å, which have been reported in our previous neutron diffraction study.[46] The tetrahedron and regular triangle are adopted as the molecular geometries of ClO_4^- and NO_3^-, respectively. The intramolecular distances are fixed at the values, $r_{ClO} = 1.43$ Å and $r_{NO} = 1.25$ Å, referred to the X-ray single crystal study of $NaClO_4 \cdot H_2O$[47] and our previous neutron diffraction work on 10 mol% $NaNO_3$–D_2O solutions[48] respectively. Values for the root-mean-square amplitudes within ClO_4^-, $l_{ClO} = 0.038$ Å and $l_{OO} = 0.059$ Å, have been calculated by means of the normal coordinate analysis[49] applying the observed frequencies for ClO_4^- in aqueous 10 mol% $NaClO_4$ solution, $\nu_1 = 937$ cm^{-1} (Raman), $\nu_2 = 1113$ cm^{-1} (Raman), $\nu_3 = 461$ cm^{-1} (Raman), and $\nu_4 = 629$ cm^{-1} (Raman). The values, $l_{NO} = 0.043$ Å and $l_{OO} = 0.050$ Å, are calculated from the vibrational frequencies, $\nu_1 = 1049$ cm^{-1} (Raman), $\nu_2 = 1404$ cm^{-1} (Raman), $\nu_3 = 717$ cm^{-1} (Raman), and $\nu_4 = 829$ cm^{-1} (IR), observed for aqueous 10 mol%

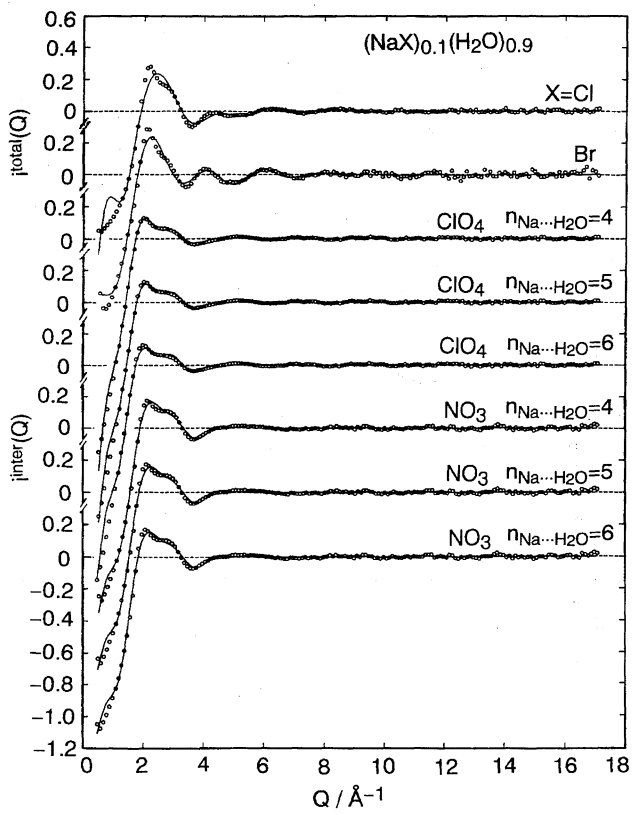

Fig. 3. Circles: Observed total and intermolecular interference terms, $i^{total}(Q)$ and $i^{inter}(Q)$, respectively, for aqueous 10 mol% NaX solutions. Solid lines: The best-fit of calculated interference terms.

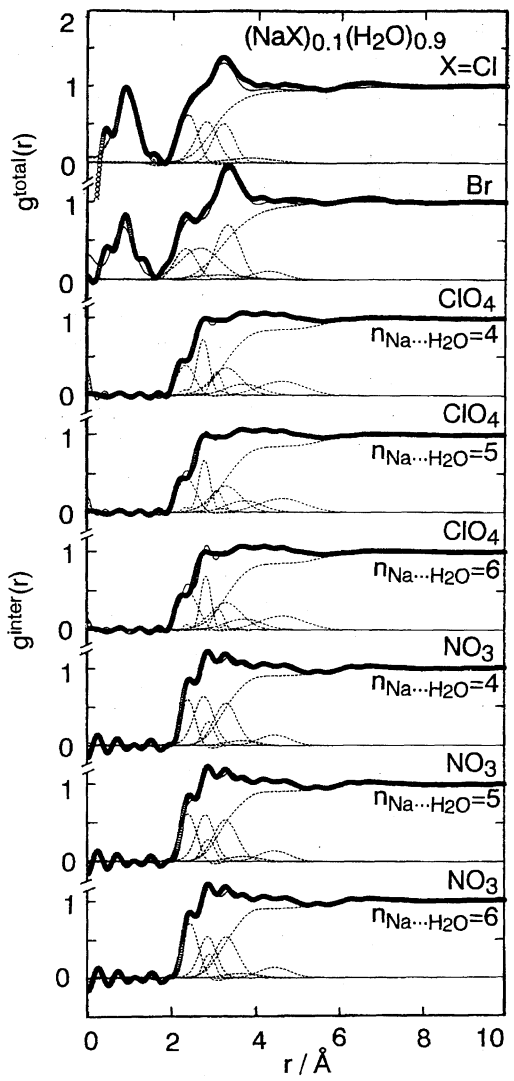

Fig. 4. Circles: Observed total and intermolecular distribution functions, $g^{total}(r)$ and $g^{inter}(r)$, respectively, for aqueous 10 mol% NaX solutions. Solid lines: The Fourier transform of the solid lines in Fig. 3. Contribution from both the short-range and long-range interactions are denoted by broken lines.

$NaNO_3$ solution. Although the nearest-neighbor ion–H_2O and H_2O–H_2O interactions should be involved in the r-range of $2<r<4$ Å in $g(r)$ for each solution, it is difficult to determine structural parameters for both interactions directly from the observed $g(r)$ because of the considerable overlapping of these interactions in r-space. Then, in order to obtain reliable values of r_{ij}, l_{ij}, and n_{ij} for the interactions, we applied the least-squares fitting analysis to the observed $i(Q)$. The following assumptions were adopted in evaluating the theoretical interference term. (a) Parameters for the nearest-neighbor $Na^+\cdots H_2O$ interaction: $r_{Na^+\cdots H_2O}$, $l_{Na^+\cdots H_2O}$, and $n_{Na^+\cdots H_2O}$ are independently refined for NaCl and NaBr solutions. The fixed values, $n_{Na^+\cdots H_2O} = 4$, 5, and 6, are adopted in the refinement procedures for both the $NaClO_4$ and $NaNO_3$ solutions. The strong correlation between the fitting parameters $n_{Na^+\cdots H_2O}$ and $n_{H_2O\cdots H_2O(I)}$ (the nearest neighbor interaction) prevents the simultaneous refinement of these parameters in the present analysis. (b) Parameters for the nearest-neighbor anion–water ($X^-\cdots H_2O$) interaction are allowed to vary independently. (c) The nearest-neighbor hydrogen-bonded $H_2O\cdots H_2O$ interaction is taken into account. Parameters $r_{H_2O\cdots H_2O(I)}$, $l_{H_2O\cdots H_2O(I)}$, and $n_{H_2O\cdots H_2O(I)}$ are independently refined. (d) The second nearest-neighbor interaction between H_2O molecules is also included in the model function.

For NaBr, $NaClO_4$, and $NaNO_3$ solutions, the contribution from the third nearest-neighbor $H_2O\cdots H_2O$ interaction is additionally involved in order to improve the fit in the lower-Q region below ca. 4 $Å^{-1}$. Since the nearest-neighbor distances for $Na^+\cdots H_2O$, $H_2O\cdots H_2O$, and $X^-\cdots H_2O$ interactions are very close to each other, it is impossible to determine structural parameters of these interactions without any assumption for initial values which are often applied to the least-squares refinement. Then literature values, $r_{Na^+\cdots H_2O}$ = 2.4 Å,[50] $r_{H_2O\cdots H_2O(I)}$ = 2.8 Å,[8—10] $r_{Cl^-\cdots H_2O}$ = 3.2 Å,[50] $r_{Br^-\cdots H_2O}$ = 3.4 Å,[50] $r_{O(ClO_4^-)\cdots H_2O}$ = 3.2 Å,[47] $r_{Cl(ClO_4^-)\cdots H_2O}$ = 3.7 Å,[47] and $r_{O(NO_3^-)\cdots H_2O}$ = 2.9 Å,[11] were respectively taken as the initial values in the fitting procedure. A reliable determination of the parameters of long-range interactions is more impossible. Then, the distance, 3 Å, was selected as the initial value of the distance parameter of r_{0ij} for atom pairs corresponding to solute–solvent and solvent–solvent interactions. The value of r_{0ij} for the solute-solute interaction was fixed at 5.6—6.0 Å because of its slight contribution. In the present analysis,

contribution from the contact ion-pair was not involved in the theoretical interference term, because of its slight contribution to the interference function, as expected from the isotropic Raman data mentioned above.

The theoretical $i(Q)$ term obtained from the best-fit model is compared with the corresponding observed one in Fig. 3. A satisfactory agreement is obtained between the observed and calculated $i^{total}(Q)$s for NaCl and NaBr solutions in the Q-range of $1 \leq Q \leq 17.1$ Å^{-1}. For both $NaClO_4$ and $NaNO_3$ solutions, theoretical $i^{inter}(Q)$s calculated for $n_{Na^+\cdots H_2O} = 4$, 5, and 6 are seem to reproduce well the observed intermolecular interference terms. Calculated and observed $g^{total}(r)$s and $g^{inter}(r)$s are compared in Fig. 4. A good agreement is again obtained for NaCl and NaBr solutions. Final results of the least-squares fitting analysis for the NaCl and NaBr solutions are listed in Table 2. Structural parameters of the $Na^+\cdots H_2O$ interaction for the concentrated NaCl solution agree well with those reported by Ohtaki and Fukushima[50] within experimental uncertainties. The hydration number of Na^+ is determined to be 4.6 for both the NaCl and NaBr solutions. For the $NaClO_4$ solution, calculated $g^{inter}(r)$ for $n_{Na^+\cdots H_2O} = 4$ well reproduces the observed one, although the $Na^+\cdots H_2O$ contribution calculated for $n_{Na^+\cdots H_2O} = 5$ and 6 seems to be obviously overestimated. The value of $n_{Na^+\cdots H_2O}$ in the present 10 mol% $NaClO_4$ solution may be close to 4. On the other hand, the calculated $g^{inter}(r)$s for $n_{Na^+\cdots H_2O} = 4$, 5, and 6 agree well with the observed $g^{inter}(r)$ for the 10 mol% $NaNO_3$ solution. The structure parameters for $NaClO_4$ and

Table 2. Results of the Least Squares Refinements for the X-Ray Interference Term of Aqueous $(NaX)_x(H_2O)_{1-x}$ Solutions (X: Cl and Br)[a]

X	x	Interaction	r_{ij}/Å	l_{ij}/Å	r_{ij}	r_{0ij}/Å	l_{0ij}/Å
Cl	0.098	$Na^+\cdots H_2O$	2.39(1)	0.21(1)	4.6(1)	3.01(2)	0.53(2)
		$Cl^-\cdots H_2O$	3.21(1)	0.27(1)	5.6(1)	3.68(2)	0.59(2)
		$H_2O\cdots H_2O$(I)	2.81(1)	0.27(1)	1.7(1)	2.93(2)	0.33(2)
		$H_2O\cdots H_2O$(II)	3.90(1)	0.55(1)	0.62(1)	—	—
		$Na^+\cdots Cl^-$					
		$Na^+\cdots Na^+$	—	—	—	6.0[b]	0.5[b]
		$Cl^-\cdots Cl^-$					
Br	0.100	$Na^+\cdots H_2O$	2.40(1)	0.23(1)	4.6(1)	3.03(2)	0.38(2)
		$Br^-\cdots H_2O$	3.38(1)	0.30(1)	5.8(1)	3.73(2)	0.43(2)
		$H_2O\cdots H_2O$(I)	2.78(1)	0.41(1)	2.8(1)	3.06(2)	0.34(2)
		$H_2O\cdots H_2O$(II)	3.23(1)	0.56(1)	0.7(1)	—	—
		$H_2O\cdots H_2O$(III)	4.36(1)	0.33(1)	1.5(1)	—	—
		$Na^+\cdots Br^-$					
		$Na^+\cdots Na^+$	—	—	—	5.6[b]	0.5[b]
		$Br^-\cdots Br^-$					

a) Estimated standard deviations are given in parentheses. b) Fixed.

Table 3. Results of the Least Squares Refinements for the X-Ray Intermolecular Interference Term of Aqueous $(NaX)_x(H_2O)_{1-x}$ Solutions (X: ClO_4 and NO_3)[a]

			$n_{Na\cdots H_2O}$=4					$n_{Na\cdots H_2O}$=5					$n_{Na\cdots H_2O}$=6				
X	x	Interaction	r_{ij}/Å	l_{ij}/Å	n_{ij}	r_{0ij}/Å	l_{0ij}/Å	r_{ij}/Å	l_{ij}/Å	n_{ij}	r_{0ij}/Å	l_{0ij}/Å	r_{ij}/Å	l_{ij}/Å	n_{ij}	r_{0ij}/Å	l_{0ij}/Å
ClO_4	0.100	$Na^+\cdots H_2O$	2.39(1)	0.21(1)	4[b]	3.23(2)	0.44(2)	2.41(1)	0.23(1)	5[b]	3.23(2)	0.47(2)	2.44(1)	0.24(1)	6[b]	3.22(2)	0.41(2)
		$O(ClO_4^-)\cdots H_2O$	3.10(1)	0.12(1)	1.2(1)	—	—	3.10(1)	0.14(1)	1.3(1)	—	—	3.14(1)	0.12(1)	1.1(1)	—	—
		$Cl(ClO_4^-)\cdots H_2O$	3.79(1)	0.43(1)	5.2(1)	3.55(2)	0.39(2)	3.81(1)	0.43(1)	5.4(1)	3.55(2)	0.39(2)	3.79(1)	0.44(1)	5.2(1)	3.55(2)	0.39(2)
		$H_2O\cdots H_2O$(I)	2.79(1)	0.12(1)	1.9(1)	3.20(2)	0.35(2)	2.82(1)	0.12(1)	1.7(1)	3.20(2)	0.35(2)	2.85(1)	0.10(1)	1.6(1)	3.22(2)	0.33(2)
		$H_2O\cdots H_2O$(II)	3.37(1)	0.34(1)	3.2(1)	—	—	3.36(1)	0.34(1)	3.1(1)	—	—	3.36(1)	0.35(1)	3.3(1)	—	—
		$H_2O\cdots H_2O$(III)	4.72(1)	0.52(1)	4.7(1)	—	—	4.72(1)	0.52(1)	4.8(1)	—	—	4.72(1)	0.52(1)	4.8(1)	—	—
		$Na^+\cdots ClO_4^-$															
		$Na^+\cdots Na^+$	—	—	—	5.7[b]	0.5[b]	—	—	—	5.7[b]	0.5[b]	—	—	—	5.7[b]	0.5[b]
		$ClO_4^-\cdots ClO_4^-$															
NO_3	0.100	$Na^+\cdots H_2O$	2.42(1)	0.17(1)	4[b]	3.37(2)	0.28(2)	2.43(1)	0.21(1)	5[b]	3.26(2)	0.28(2)	2.45(1)	0.21(1)	6[b]	3.34(2)	0.28(2)
		$O(NO_3^-)\cdots H_2O$	2.90(1)	0.14(1)	1.3(1)	—	—	2.89(1)	0.15(1)	1.3(1)	—	—	2.89(1)	0.13(1)	1.3(1)	—	—
		$N(NO_3^-)\cdots H_2O$	3.71(1)	0.36(1)	4.0(1)	3.64(2)	0.28(2)	3.76(1)	0.37(1)	4.3(1)	3.67(2)	0.28(2)	3.71(1)	0.39(1)	4.1(1)	3.64(2)	0.28(2)
		$H_2O\cdots H_2O$(I)	2.80(1)	0.22(1)	2.2(1)	3.06(2)	0.25(2)	2.83(1)	0.20(1)	2.0(1)	3.05(2)	0.25(2)	2.87(1)	0.19(1)	1.8(1)	3.06(2)	0.24(2)
		$H_2O\cdots H_2O$(II)	3.32(1)	0.27(1)	3.2(1)	—	—	3.32(1)	0.27(1)	3.2(1)	—	—	3.32(1)	0.27(1)	3.2(1)	—	—
		$H_2O\cdots H_2O$(III)	4.48(1)	0.35(1)	1.9(1)	—	—	4.48(1)	0.35(1)	1.9(1)	—	—	4.48(1)	0.36(1)	1.9(1)	—	—
		$Na^+\cdots NO_3^-$															
		$Na^+\cdots Na^+$	—	—	—	5.7[b]	0.4[b]	—	—	—	5.7[b]	0.4[b]	—	—	—	5.7[b]	0.4[b]
		$NO_3^-\cdots NO_3^-$															

a) Estimated standard deviations are given in parentheses. b) Fixed.

$NaNO_3$ solutions are summarized in Table 3. The value of the nearest-neighbor $Na^+\cdots H_2O$ distance, $r_{Na^+\cdots H_2O}$ = 2.39 and 2.42 Å, respectively obtained from the present $NaClO_4$ and $NaNO_3$ solutions for the fixed $n_{Na^+\cdots H_2O}$ value of 4, are in reasonable agreement with those obtained for the 10 mol% NaCl and NaBr solutions. A systematic increase in the value of $r_{Na^+\cdots H_2O}$ can be observed with increasing $n_{Na^+\cdots H_2O}$ from 4 to 6 for the present $NaClO_4$ and $NaNO_3$ solutions. Considering the anion-independent ν_1 frequency for the present NaX solutions, the value of $r_{Na^+\cdots H_2O}$ obtained for $n_{Na^+\cdots H_2O}$ = 4 is considered to be more reliable than that for $n_{Na^+\cdots H_2O}$ = 5 and 6 for the present 10 mol% $NaNO_3$ solution. Additionally, the observed value of $l_{Na^+\cdots H_2O}$, 0.17—0.23 Å, is roughly consistent with the value $l_{Na^+\cdots H_2O}$ = 0.15 Å, which is calculated from the observed symmetrical stretching vibrational frequency, ν_1 = 183 cm^{-1}, observed in the present Raman data, assuming the tetrahedral geometry of the hydrated Na^+. The hydration number of Na^+ in the present 10 mol% NaX solutions (X: Cl, Br, ClO_4, and NO_3) is then concluded to be close to 4. A concentration-dependent hydration number of alkali metal ions has often been suggested in the literature.[50] It may be of interest to investigate the concentration dependence of the hydration structure of Na^+ in the aqueous solution. This will be a near-future subject.

Structural information concerning the hydration structure of polyatomic anions such as ClO_4^- and NO_3^- can be deduced from the present X-ray data. The distance between $O(ClO_4^-)$ atom and H_2O molecule, 3.10 Å, in the first hydration shell around ClO_4^- is ca. 0.3 Å longer than the nearest-neighbor hydrogen-bonded $H_2O\cdots H_2O$ distance in the same solution, implying the weaker $O(ClO_4^-)\cdots H_2O$ interaction in the solution. The present $O(ClO_4^-)\cdots H_2O$ distance is in good agreement with 3.05 Å, the value predicted from infrared double difference spectra.[51] The nearest-neighbor $Cl(ClO_4^-)\cdots H_2O$ distance, 3.79 Å, is consistent with ca. 3.7 Å reported by the neutron diffraction study with the $^{35}Cl/^{37}Cl$ isotopic substitution method.[52] In this result, each O atom within ClO_4^- in the aqueous 10 mol% $NaClO_4$ solution bonds to, on the average, one H_2O molecule with the bond angle of $\angle Cl\text{–}O\cdots H_2O = 108\pm2°$.

The nearest- neighbor $N(NO_3^-)\cdots H_2O$ distance, 3.71±0.01 Å, roughly agrees with 3.78 Å obtained by neutron diffraction data.[48] The distance $O(NO_3^-)\cdots H_2O$, 2.90 Å, is ca. 0.1 Å longer than the nearest-neighbor hydrogen-bonded $H_2O\cdots H_2O$ distance. We conclude that each O atom within NO_3^- in the aqueous 10 mol% $NaNO_3$ solution forms the hydrogen bond with the nearest-neighbor H_2O molecule with the calculated bond-angle, $\angle N\text{–}O\cdots H_2O = 122\pm2°$.

The authors wish to thank Professor George E. Walrafen (Howard University), Professor Murray H. Brooker (Memorial University of Newfoundland) and Dr. Hiroshi Takeuchi (Hokkaido University) for their helpful discussions. All of the calculation in this work were carried out with the S-4/1000 computer at the Computing Center of Yamagata University. This work was partially supported by a Grant-in-Aid for Scientific Research No. 09640657 from the Ministry of Education, Science, Sports and Culture.

References

1) R. M. Lawrence and R. F. Kruh, *J. Chem. Phys.*, **47**, 4758 (1967).
2) G. Licheri, G. Piccaluga, and G. Pinna, *J. Appl. Cryst.*, **6**, 392 (1972).
3) M. Maeda and H. Ohtaki, *Bull. Chem. Soc. Jpn.*, **48**, 3755 (1975).
4) R. Caminiti, G. Licheri, G. Piccaluga, and G. Pinna, *Rend. Semin. Fac. Sci. Univ. Cagliari*, **47**, 19 (1977).
5) G. Pálinkás, W. O. Riede, and K. Heinzinger, *Z. Naturforsch., A*, **32a**, 1137 (1977).
6) G. Pálinkás, T. Radnai, and F. Hajdu, *Z. Naturforsch., A*, **35a**, 107 (1980).
7) R. Caminiti, F. Cilloco, and R. Felici, *Mol. Phys.*, **76**, 681 (1992).
8) H. Ohtaki and N. Fukushima, *J. Solution Chem.*, **21**, 23 (1992).
9) Y. Kameda, R. Takahashi, T. Usuki, and O. Uemura, *Bull. Chem. Soc. Jpn.*, **67**, 956 (1994).
10) Y. Kameda, T. Mori, T. Nishiyama, T. Usuki, and O. Uemura, *Bull. Chem. Soc. Jpn.*, **69**, 1495 (1996).
11) R. Caminiti, G. Licheri, G. Paschina, G. Piccaluga, and G. Pinna, *J. Chem. Phys.*, **72**, 4522 (1980).
12) N. Ohtomo and K. Arakawa, *Bull. Chem. Soc. Jpn.*, **53**, 1789 (1980).
13) N. T. Skipper and G. W. Neilson, *J. Phys: Condens. Matter*, **1**, 4141 (1989).
14) G. Heinje, W. A. P. Luck, and K. Heinzinger, *J. Phys. Chem.*, **91**, 331 (1987).
15) E. Guàrdia and J. A. Radró, *J. Phys. Chem.*, **94**, 6049 (1990).
16) G. Hummer and D. M. Soumpasis, *Mol. Phys.*, **75**, 633 (1992).
17) J. Gao, *J. Phys. Chem.*, **98**, 6049 (1994).
18) D. A. Dráegert and D. Williams, *J. Chem. Phys.*, **48**, 401 (1968).
19) H. R. Zelsmann, *J. Mol. Struct.*, **350**, 95 (1995).
20) T. Tassaing, Y. Danten, M. Besnard, E. Zoidis, J. Yarwood, Y. Guissani, and B. Guillot, *Mol. Phys.*, **84**, 769 (1995).
21) G. E. Walrafen, *J. Chem. Phys.*, **36**, 1035 (1962).
22) G. E. Walrafen, *J. Chem. Phys.*, **40**, 3249 (1964).
23) G. E. Walrafen, "Water, A Comprehensive Treatise," ed by F. Franks, Prenum Press, New York (1972), Vol. 1, p. 151.
24) M. Moskovits and K. H. Michaelian, *J. Chem. Phys.*, **69**, 2306 (1978).
25) G. E. Walrafen, M. R. Fisher, M. S. Hokmabadi, and W.-H. Yang, *J. Chem. Phys.*, **85**, 6970 (1986).
26) G. E. Walrafen, M. S. Hokmabadi, W.-H. Yang, Y. C. Chu, and B. Monosmith, *J. Phys. Chem.*, **93**, 2909 (1989).
27) M. H. Brooker, G. Hancock, B. C. Rice, and J. Shapter, *J. Raman Spectrosc.*, **20**, 683 (1989).
28) P. Terpsta, D. Combes, and A. Zwick, *J. Chem. Phys.*, **92**, 65 (1990).
29) G. E. Walrafen, Y. C. Chu, and G. J. Piermarini, *J. Phys. Chem.*, **100**, 10363 (1996).
30) H. Kanno and J. Hiraishi, *J. Phys. Chem.*, **88**, 2787 (1984).
31) M. H. Brooker, "The Chemical Physics of Solvation, Part B," ed by R. R. Dogonadze, E. Kalman, A. A. Kornyshev, and J. Ulstrup, Elsevier, Amsterdam, Chap. 4, p. 119.
32) H. Kanno, *Bull. Chem. Soc. Jpn.*, **59**, 3651 (1986).

33) H. Kanno, *J. Phys. Chem.*, **92**, 4232 (1988).
34) H. Kanno, T. Yamaguchi, and H. Ohtaki, *J. Phys. Chem.*, **93**, 1695 (1989).
35) W. Rudolph and G. Irmer, *J. Solution Chem.*, **23**, 663 (1994).
36) K. H. Michaelian and M. Moskovits, *Nature*, **273**, 135 (1978).
37) Y. Kameda, H. Ebata, and O. Uemura, *Bull. Chem. Soc. Jpn.*, **67**, 929 (1994).
38) W. Rudolph, M. H. Brooker, and C. C. Pye, *J. Phys. Chem.*, **99**, 3793 (1995).
39) Y. Kameda, I. Sugawara, K. Kijima, T. Usuki, and O. Uemura, *Bull. Chem. Soc. Jpn.*, **68**, 512 (1995).
40) G. W. Chantry, "The Raman Effect," ed by A. Anderson, Marcel Dekker Inc., New York (1971), Vol. 1, p. 70.
41) J. R. Scherer, M. K. Go, and S. Kint, *J. Phys. Chem.*, **79**, 913 (1975).
42) M. Lucas, A. De Trobriand, and M. Ceccaldi, *J. Phys. Chem.*, **79**, 913 (1975).
43) T. Nakagawa and Y. Oyanagi, "Recent Developments in Statistical Inference and Data Analysis," ed by K. Matushita, North-Holland (1980), p. 221.
44) A. H. Narten, M. D. Danford, and H. A. Levy, *Discuss. Faraday Soc.*, **43**, 97 (1967).
45) R. Caminiti, P. Cucca, M. Monduzzi, G. Saba, and G. Crisponi, *J. Chem. Phys.*, **81**, 543 (1984).
46) Y. Kameda and O. Uemura, *Bull. Chem. Soc. Jpn.*, **65**, 2021 (1992).
47) B. Berglund, R. Tellgren, and J. O. Thomas, *Acta Crystallogr., Sect. B*, **B32**, 2444 (1976).
48) Y. Kameda, H. Saitoh, and O. Uemura, *Bull. Chem. Soc. Jpn.*, **66**, 1919 (1993).
49) S. J. Cyvin, "Molecular Vibrations and Mean Square Amplitudes," Elsevier, Amsterdam (1968) Chap. 7, p. 196.
50) H. Ohtaki and T. Radnai, *Chem. Rev.*, **93**, 1157 (1993).
51) O. Kristiansson, A. Eriksson, and J. Lindgren, *Acta Chem. Scand., Ser. A*, **A38**, 609 (1984).
52) G. W. Neilson, D. Schiöberg, and W. P. A. Luck, *Chem. Phys. Lett.*, **122**, 475 (1985).